

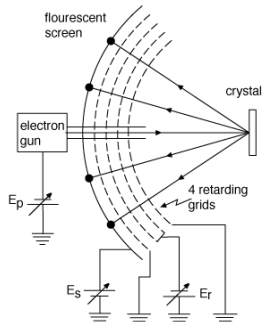
Lesson 07

Experimental diffraction techniques

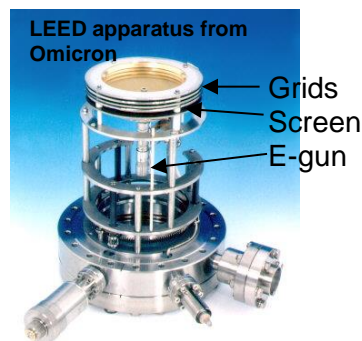
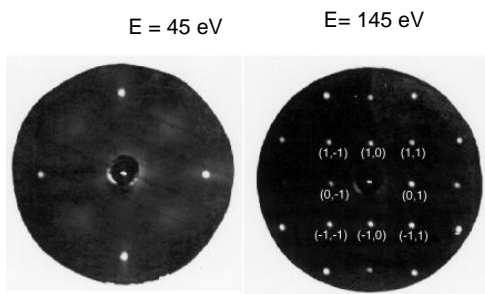
Low Energy Electron Diffraction (LEED)

Electron beams for surface studies are relatively easy to produce. A heated tungsten filament and a few electrostatic lenses are sufficient for the production of a good quality electron beam. The energy width δE of the beam is equal to kT , where T is the temperature of the filament. For $T=2000\text{ K}$, $\delta E \sim 0.2\text{ eV}$. A typical beam energy range is 20 to 500 eV, sufficient to cover most lattice periodicities in solid surfaces. The spot size is typically less than one millimeter in diameter. Nowadays it is possible to generate spot sizes in the micrometer range, and even lower, particularly at high energies. At the lowest energy, space charge repulsion prevents the beam from being focused to a very small spot. The beam current is in the nano- to microampere range, although lower currents are possible and desirable to minimize damage to the surface, particularly with ionic surfaces and surfaces that contain organic molecules, which are sensitive to electron beam damage. Low current also facilitates discharge of the surface, which is necessary for insulators. In that case currents in the picoampere range can be used. This corresponds to arrival frequencies of $10^{-12} \times 10^{19}\text{ s}^{-1} = 10^7\text{ s}^{-1}$, or time intervals between electrons of 10^{-7} s . Since the lifetime of a trapped charge is easily lower than 1 microsecond, the charging problem is minimized.

The LEED apparatus:



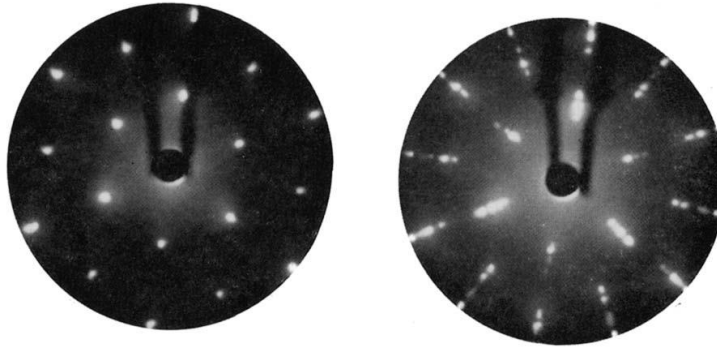
Example of diffraction patterns of a W (100) surface at two different electron energies



A LEED diffractometer usually consists of four concentric grids and a phosphorescent screen. The most external one (first grid) is grounded. It provides an electrical field-free space for the diffracted electrons, so that their trajectories are not altered. Care must also be taken to avoid stray magnetic fields, particularly at the lowest electron energies. The middle grids are connected together to a repulsive potential. This repels the electrons that have lost more than a few eV's of energy. The fourth or innermost grid is usually grounded, while the screen is polarized to several thousand volts (positive). This accelerates the electrons to an energy suitable to excite fluorescence of the material coating the screen. Nowadays, channel plates often substitute for the screen. This allows for digital data collection, as well as provide a large amplification which makes it easy (and necessary) to work with low beam currents.

Exercise: What diffracted beams will be captured in the screen of 10 cm radius with the sample located at the center as a function of energy?

SURFACE SCIENCE 11 (1968) 82-98 Q North-Holland Publishing Co., Amsterdam
LEED FROM SURFACE STEPS ON UO_2 SINGLE CRYSTALS*
W. P. ELLIS
Los Alamos Scientific Laboratory, University of California,
Los Alamos, New Mexico 81544, U.S.A. and R. L. SCHWOBEL
Sandia Laboratory, Albuquerque, New Mexico 87115, U.S.A.
Received 8 December 1967; revised manuscript received 18 January 1968



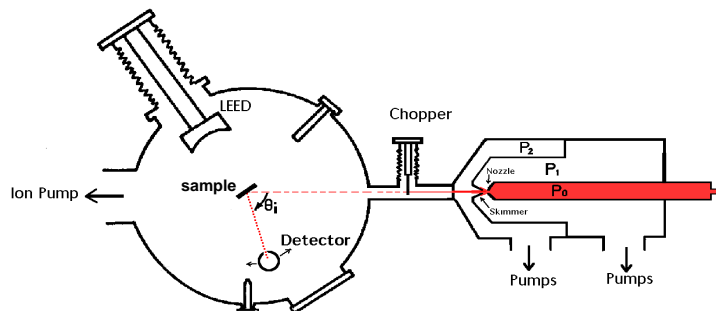
Pattern from "clean" UO_2 (111) at 128 eV. The (00) beam is hidden by the electron gun; only integral-order beams are seen. (b) Multiple exposure at various beam energies showing convergence of the integral order spots to the (00) reflection of the UO_2 (111) with increasing voltage.

Atom scattering

Beams of atoms for diffraction studies are a bit more difficult to produce. The following is a schematic of an apparatus to produce beams of atoms or molecules. The gas is contained in a stagnation chamber at a pressure P_0 and allowed to expand through an orifice (nozzle). If P_0 is in the less than 1 torr, the mean free path is larger than the dimensions of the orifice (~ 1 mm). The source is called effusive and the velocity distribution is given by the Maxwell distribution corresponding to the chamber temperature T_0 . The beam emerges with a cosine distribution of directions at the exit:

$$dI(\theta, r) = \frac{d\Omega}{4\pi} n \bar{v} A \cos \theta \quad (9)$$

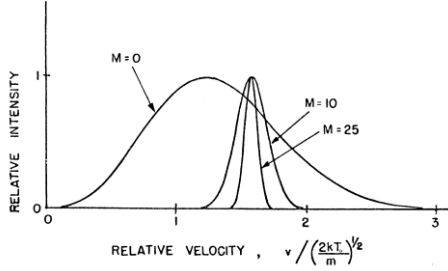
where n is the gas density ($=P_0/RT$) and \bar{v} the mean molecular velocity. The flux is of 4×10^{16} particles $\text{sr}^{-1} \text{sec}^{-1}$ at 300K. At 1 meter distance this corresponds to a beam intensity of 5×10^{12} particles $\text{cm}^{-2} \text{sec}^{-1}$. If a slotted disk pair is used for velocity selection this dramatically reduces the intensity.



A better solution is to use supersonic nozzle beam sources. Here P_0 is much higher than 1 torr (up to several 10's atmospheres), so that the mean free path λ , is much smaller than the diameter of the nozzle d . When the Knudsen number $K = \lambda/d$ decreases well below

unity the intensity of the beam increases linearly with source pressure up to values of $K \sim 10^{-3}$. This corresponds to continuum flow in the orifice followed by molecular flow, as the beam density decreases far from the orifice. A sharp edged conical skimmer selects the central portion of the beam. Kantrowicz and Grey studied the properties of these sources. They found that the velocity distribution at the skimmer entrance is given by:

$$I(u, v, w) du dv dw = \left(\frac{m}{2\pi k T_s} \right)^{3/2} \left[e^{-\frac{m}{2k T_s} ((v-v_s)^2 + u^2 + w^2)} \right] du dv dw \quad (10)$$



i.e., a shifted Maxwell distribution, where v_s is the flow velocity of the beam, v the velocity along the beam axis and u and w the perpendicular components. T_s is the temperature at the skimmer entrance. This differs from effusive sources in that v_s is not zero. As a function of the Mach number $M = v_s/c$ (c = local sound velocity given by

$$\sqrt{\frac{\gamma T_s}{m}} \text{ where } \gamma = \frac{c_p}{c_v}, \text{ the ratio of heat capacities),}$$

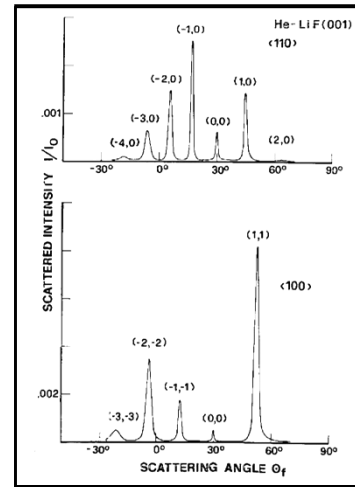
the velocity distribution has a maximum shifted to higher values than that of the effusive source. It is also narrower, as shown in the figure. If we define a velocity ratio

$$S = \sqrt{\frac{mv_s^2}{2kT}}, \text{ where } T \text{ is the temperature describing the mean kinetic energy of the}$$

molecular motion in the gas which moves with flow velocity v_s . The important properties of the beam: fwhm of the velocity distribution and temperature T are given by:

$\Delta v/v_s = 1.65/S$; and $T/T_0 = 2.5/S^2$. T_0 is the temperature of the stationary gas before expansion. So the beam becomes more monoenergetic and cooler. This leads to many interesting phenomena, in addition to their usefulness for diffraction and scattering. Clusters may condense along the beam, where T can reach values of a few K. The intensities can be very high, of the order of 10^{20} particles $\text{sr}^{-1} \text{sec}^{-1}$, four orders of magnitude higher than for effusive beams, even before monochromatization!.

Example of He diffraction off a LiF surface, obtained by Boato et al. (ref.):



Nomenclature of diffraction patterns: reciprocal and real spaces

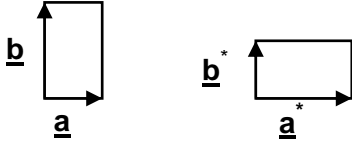
If \underline{a} and \underline{b} are the unit cell vectors of the real space 2-D lattice and if \underline{c} is a vector perpendicular to the surface of unit length, the reciprocal lattice unit cell vectors \underline{a}^* and \underline{b}^* are defined by the following relations:

$$\vec{a}^* = 2\pi \frac{\vec{b} \times \vec{c}}{V}, \quad \vec{b}^* = 2\pi \frac{\vec{c} \times \vec{a}}{V}; \quad (1)$$

the volume V being $= \underline{a} \cdot (\underline{b} \times \underline{c})$. This is equivalent to the following set of conditions:

$$\left. \begin{array}{l} \underline{a} \cdot \underline{a}^* = 2\pi \\ \underline{a} \cdot \underline{b}^* = 0 \\ \underline{a}^* \cdot \underline{b} = 0 \\ \underline{b} \cdot \underline{b}^* = 2\pi \end{array} \right\} \quad (2)$$

Rectangular lattice



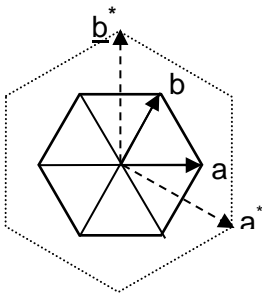
If we write $\underline{a}^* = p \underline{a}$, and $\underline{b}^* = q \underline{b}$, the conditions (2) imply:

$$p = 2\pi/a^2 \text{ and } q = 2\pi/b^2.$$

Therefore the length of \underline{a}^* and \underline{b}^* are $2\pi/a$ and $2\pi/b$.

Hexagonal lattice

The drawing shows the relative orientations of the unit cell vectors \underline{a}^* and \underline{b}^* which are perpendicular to \underline{b} and \underline{a} respectively. From (13) we can write:



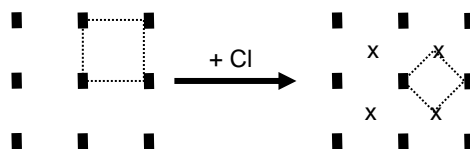
$$|\vec{a}| \cdot |\vec{a}^*| \cdot \cos 30 = 2\pi \quad (3)$$

and a similar expression for \underline{b} . The length of the reciprocal lattice vector is then:

$$|\vec{a}^*| = \frac{4\pi}{\sqrt{3} \cdot a}$$

From reciprocal to real space

When chlorine adsorbs on Cu(100) the LEED pattern changes as shown in the drawing: a new diffraction spot appears at the center of each cell. The new unit cell vectors (dashed lines) are $\sqrt{2}$ times smaller in reciprocal space and rotated by 45° .

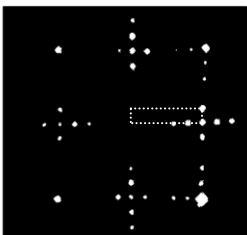
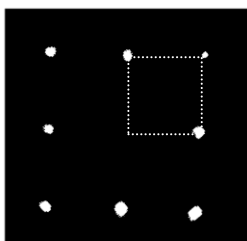


In real space the new unit cell will also be a square rotated 45° but $\sqrt{2}$ larger. The nomenclature is $(\sqrt{2} \times \sqrt{2})R45^\circ$. Another notation is sometimes used that involves non-primitive cells. For example, the same chlorine structure can be labeled as $c(2 \times 2)$, the c standing for “centered”. The use of centered unit cells is convenient because of its simplicity.

Of course we do not know the position of the chlorine atoms. The Cl atoms can be located at the center, between 4 Cu atoms, the so-called four-fold position, or any other position. For example we can move the Cl atom to the top position (above a Cu atom), to bridge positions (between 2 Cu atoms) or anywhere else. There could also be more than one atom in each cell. In other words the content of the unit cell cannot be obtained only from the periodicity seen in the LEED pattern. For that a theory of the diffracted intensities is necessary, as discussed in the previous lesson.

Domains

On many surfaces several directions are physically equivalent. For example the (01) and (10) directions of a square lattice are undistinguishable. In hexagonal lattices, like the (111) surfaces of cubic crystals and the (0001) surfaces of hexagonal crystals, there are 3 equivalent directions. In these surfaces, the structure formed for example by adsorption of atoms and molecules can appear in two, three, or more domains that are only rotationally different. The unit cell vectors of their periodical arrangements will be also rotated. That means that a diffraction pattern will consist in the superposition of the diffraction patterns of each domain. That can lead to sometime difficult to interpret patterns.



For example, the $m \times 1$ and $1 \times m$ structures are characterized by the appearance of extra spots on the sides of the original unit cell, m in one direction and n in the other. This is the case of the 5×1 structure of reconstructed Ir, Au and Pt (100) surfaces (in the last two cases it is not exactly 5×1). Another domain rotated 90° will also appear and the LEED pattern will be a superposition of the two.

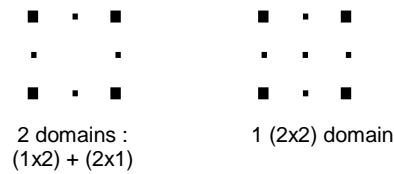
Example: Ir(100), Top: metastable 1×1 (unit cell in broken lines). Bottom: reconstructed (1×5) (from K. Müller and K.



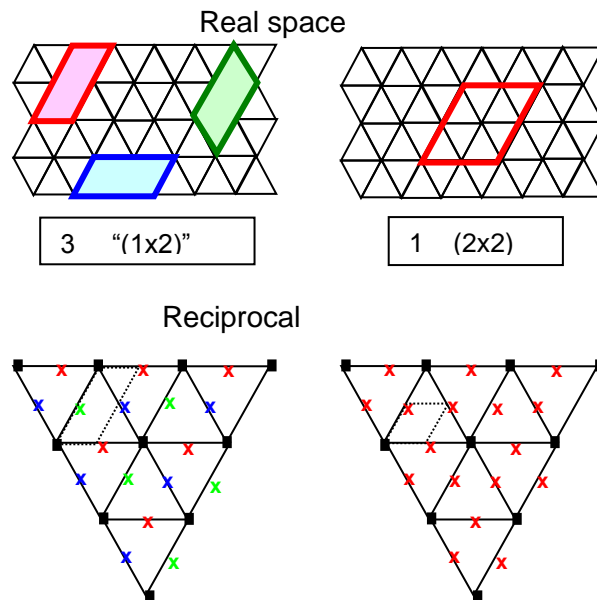
Heinz). The unit cell of one of the domains is drawn in broken lines. This reconstruction is the result of a densification of the surface. The top layer adopts the structure of a (111) hexagonal plane, overlaid on top of the (100) plane such that one compact direction of the hexagonal plane coincides with the side of the square. The coincidence in the other

direction is then $6 \times \frac{\sqrt{3}}{2} = 5$, (within 4%). The surface is 15% denser than the unreconstructed 1x1.

For square and rectangular lattices, there is no confusion between 2 domains of 2x1 symmetry and one of 2x2 symmetry. Their patterns look like:



On hexagonal surfaces, like the (0001) basal plane of hcp systems and the (111) face of



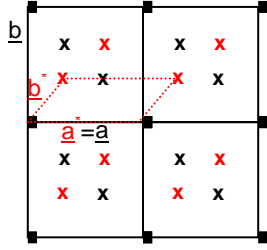
fcc systems a potential ambiguity exists. The figure shows in real space, three 1x2 domains on the left, and one 2x2 domain on the right. The corresponding LEED patterns are shown below in schematic form. The left pattern has three different sets of spots (three colors), one for each domain rotated 120°. The one on the right has only one. As can be seen, they look identical.

If the coverage θ is known then one of them can be excluded. For example if $\theta = 0.5$, then the structure must be a mixture of (1x2)-type orientations. If $\theta = 0.25$, then it could be a (2x2) fully covering the surface, or a surface half covered by a 2x1 structure. In

some cases bitter controversies only recently resolved have arisen because θ is not known, or the error bar is too large. This is the case of CO on Pt(111) for example.

Matrix notation

Sometimes it is not possible to express in a simple (nxm) notation (so called Wood notation) the unit cell vectors in terms of those of the ideal, clean surface. In this case a 2x2 matrix notation is used, with each row containing the x and y coordinates of the new lattice unit cell vectors. The following example, corresponding to S/Mo(100) at 2/3 coverage, illustrates this:



The crosses represent the new diffraction spots that appear when S is adsorbed. There are two domains producing spots in red and black. The red ones for example, can be expressed as a function of the old ones \underline{a}^* and \underline{b}^* as:

$$\underline{a}'^* = \underline{a}^* \text{ and } \underline{b}'^* = 1/3 \underline{a}^* + 2/3 \underline{b}^*, \text{ with } \mathbf{M} = \begin{bmatrix} 1 & 0 \\ 1/3 & 2/3 \end{bmatrix}$$

To obtain the coefficients connecting the new real space unit cell vectors \underline{a}' and \underline{b}' to \underline{a} and \underline{b} , we just need to invert the matrix \mathbf{M} . This can be seen as follows. First we express in matrix notation the above relation between the new and old reciprocal lattice vectors (vectors in a matrix represent the rows of its coordinates).

$$\begin{pmatrix} \underline{a}'^* \\ \underline{b}'^* \end{pmatrix} = \mathbf{M} \cdot \begin{pmatrix} \underline{a}^* \\ \underline{b}^* \end{pmatrix} \quad (15)$$

Next we multiply from the left by $(\underline{a}', \underline{b}')$ (this again represents a matrix with columns equal to the coordinates of \underline{a}' and \underline{b}' . This time of course we use the conjugate form).

$$(\underline{a}' \quad \underline{b}') \begin{pmatrix} \underline{a}'^* \\ \underline{b}'^* \end{pmatrix} = (\underline{a}' \quad \underline{b}') \mathbf{M} \begin{pmatrix} \underline{a}^* \\ \underline{b}^* \end{pmatrix}$$

From (13), we know that the product on the left hand side is just $2\pi \cdot \mathbf{I}$, where \mathbf{I} is the identity matrix. Next we multiply from the right by $(\underline{a}, \underline{b})$, and again using (13) we get on the right $2\pi \cdot \mathbf{I}$

$$(\underline{a} \quad \underline{b}) = (\underline{a}' \quad \underline{b}') \mathbf{M}$$

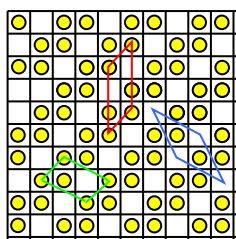
Where we have eliminated the two $2\pi \cdot \mathbf{I}$'s. Then we multiply from the right by \mathbf{M}^{-1} , the inverse matrix. We get finally:

$$\begin{pmatrix} \vec{a}' & \vec{b}' \end{pmatrix} = \begin{pmatrix} \vec{a} & \vec{b} \end{pmatrix} \mathbf{M}^{-1}$$

or, transposing rows and columns:

$$\begin{pmatrix} \vec{a}' \\ \vec{b}' \end{pmatrix} = \mathbf{M}^{-1} \cdot \begin{pmatrix} \vec{a} \\ \vec{b} \end{pmatrix} \quad (16)$$

In the previous example of the sulfur on Mo(100), $\det[\mathbf{M}] = 1/3$ and $\mathbf{M}^{-1} = \begin{pmatrix} 1 & -1 \\ 0 & 3 \end{pmatrix}$, is



the matrix we sought. There are as we know infinite ways to choose a primitive cell. All others can be obtained by adding to one row of \mathbf{M}^{-1} , any multiple of the other row. For example adding the first to the second gives $\begin{pmatrix} 1 & -1 \\ 1 & 2 \end{pmatrix}$, which is another perfectly valid notation for the same structure.

The structure in real space shown on the left schematic was proposed (using the known value $\theta = 0.67$) to be the solution. The yellow balls represent sulfur atoms sitting on four-fold coordinated sites of the Mo(100) lattice. Three possible choices of the unit cell are drawn. This structure was later confirmed by STM imaging.

<http://www.ap.cityu.edu.hk/personal-website/Van-Hove.htm>

On-line interactive software

- **Photoelectron Diffraction** intensity computation (PED): [EDAC](#) (some restrictions apply; by F.J. García de Abajo)
- **Visualizer of bulk-terminated crystalline surface structures**: [Surface Explorer](#) on-line (by F. Hammer and K. Hermann) [Back](#)

Software for download (all free):

- **Graphical LEED pattern simulator**: [LEEDpat](#) (executable for Windows; by K. Hermann and F. Hammer; on-line version also available: see above)
- **Low-Energy Electron Diffraction** intensity computation, **with phase shift calculation and data**: [LEED](#), including conventional LEED, ATLEED, SATLEED, SATCLEED, MSATLEED, ATLMLEED (FORTRAN source code; by M.A. Van Hove, J.B. Pendry, S.Y. Tong, P.J. Rous, A. Wander, A. Barbieri, G. Ketteler et al)
- **Photoelectron Diffraction** intensity computation (PED): [MSCD](#) (C++ source code and executables; by Y. Chen)

- **Atomic-Scale Holography with Photoelectrons (PEH) and X-rays (XRH):** [Holographic package](#) for atomic-scale reconstruction (FORTRAN source code; by P.M. Len)

- **Relaxation Energies in Photoemission:** [REPS](#) (C++ source code; by Y. Chen)

- **Surface graphics software:** [SARCH, LATUSE, PLOT3D package](#) (executables for DOS; by M.A. Van Hove and K. Hermann)

Database of surface structures:

- **Surface Structure Database:** [SSD](#) (executable for Windows; by P.R. Watson, M.A. Van Hove and K. Hermann) sold by NIST